Light scattering investigation of 2D and 3D opal template formation on hydrophilized surfaces

E. Armstrong[1], W. Khunsin[2], M. Osiak[1], C. M. Sotomayor Torres[2,3], and C. O'Dwyer[1,4]

[1]*Department of Chemistry, University College Cork, Cork, Ireland*
[2]*Catalan Institute of Nanoscience and Nanotechnology ICN2, Campus UAB, Edifici ICN2, 08193 Bellaterra, Spain*
[3]*Catalan Institute for Research and Advances Studies (ICREA), 08010 Barcelona, Spain*
[4]*Micro and Nanoelectronics Centre, Tyndall National Institute, Lee Maltings, Cork, Ireland*

We demonstrate the formation of 2D photonic crystals (opals) on gold coated silicon substrates by dip-coating at a high rate of 1 mm/min when the surfactant sodium dodecyl sulphate (SDS) is added to the solution above its critical micelle concentration. The dependence of substrate hydrophillicity is demonstrated to influence the formation of 3D templates on glass substrates using 700 nm diameter PMMA spheres. Other routes towards directing opal assembly are also discussed. Angle-resolved reflectance shows 2D and 3D light scattering characteristics from the fast-rate dip-coated monolayer 2D 3D photonic crystals grown on hydrophillized glass respectively, with a high degree of surface ordering.

Introduction

Photonic crystals are aperiodic dielectric materials with a periodicity on the scale of the wavelength of light.(1) These can occur naturally in nature, for example, in certain butterfly wings, bird feathers and in opal stones.(2, 3) They influence the flow of light, forbidding the propagation of certain wavelengths depending on its porosity and refractive index, much like a semiconductor controls the flow of electrons. This light is then transmitted or reflected from the material at particular angles giving rise to the colors observed in opals. Synthetic opals are an ordered assembly of nanometer sized silica spheres and therefore can be artificially formed through the self-assembly of mono-dispersed colloidal particles, such as, silica spheres or polymer spheres of polystyrene (PS) or poly(methylmethacrylate) (PMMA).

Photonic crystals (PhCs) have been heavily investigated over the last 50 years due to the wide-range of their optical characteristics and design potential and therefore, their possible application in numerous fields of science and engineering. They have been adopted as reliable means for forming two-dimensional (2D) and three-dimensional(3D) ordered structures(4), useful as optical waveguides(5), switches(6), light-emitting diodes(7). They can also function as templates, particularly on non-planar substrates, for the formation of these and other functional materials,(8, 9) such as battery electrodes(10, 11). By assembling spheres (silica or polymer-based) in ordered 2 or 3 dimensional arrangements it is possible to mimic the iridescence of natural opals and so create a material in which you can control the photonic and optical properties. Assembly of these arrays of spheres is done through a variety of means(1), drop-casting of the sphere solution(12), dip coating(13, 14), spin coating(15),vertical deposition(16), electrophoretic deposition(17), Langmuir-Blodgett(18, 19) or layer-by-layer assembly(20).

The control that dip-coating in particular, allows towards evaporation rate and meniscus control makes it one of the more highly utilized techniques, due to its ability to

form well-ordered multilayer deposits of spheres when used at a slow rate of withdrawal and its potential for application in an industrial setting(14). Improvement in the coverage and long-range order of deposits can be achieved through the control and/or the addition of other variables such as temperature(21), management of the ionic strength of the solution via the use of charged colloids(22), or noise-induced stochastic resonance effects.(23) We briefly investigate the formation of 3D PhCs on glass substrates by dip-coating of 500 nm PS spheres with noise induced stochastic resonance. We show the importance of hydrophillized surfaces for the initial absorption of the spheres onto the substrate and the level of long range order they exhibit.

However, one of the more emerging fields of use for these opal templates is their use in the formation of metal dielectric interfaces, which have been seen to reduce coupled light leakage(24, 25), improve the quality factor for index-guided optical modes(26), and improve overall performance, for potential application in enhanced solar cells, light emitters and gas sensors(26, 27), respectively. Therefore, an important step in defining the optical properties and application of these hybrid plasmonic-photonic crystals is the formation of opal templates on metallic surfaces, particularly those capable of holding surface plasmon polaritions (SPPs). Under ambient conditions however coating of gold surfaces is difficult due to the effects carbonaceous contamination has on clean gold surfaces, turning them from naturally hydrophilic to hydrophobic on interaction with air(28). This induces disorder on most templates formed on gold substrates when assembled in air, however, we will show the formation of highly ordered 2D photonic crystal (PhC) monolayers on gold substrates by dip-coating when a surfactant, sodium dodecyl sulphate, is first added to the solution of spheres. In addition, we discuss the formation of multi-layer 2D PhC templates, with a similar scattering ability to the monolayer template, at a slower rate of withdrawal when the sphere and surfactant concentration are reduced. We use light scattering and scanning electron microscopy (SEM) to determine the order in the samples. Reflectance from a true 3D opal is related to its film thickness via Bragg attenuation length and therefore, we refer to the photonic crystals with thickness of a few monolayers as principally 2D structures due to the absence of 3D-related optical characteristics. The Bragg attenuation length for our PHCs assembled from 700 nm diameter PMMA spheres is of the order of 6.5 to 7 um or approximately 12 monolayers of spheres(29).

Experimental

Glass substrates were prepared by two methods. In the first, a glass substrate was submerged for approximately 5 minutes in Piranha solution, prepared using hydrogen peroxide and sulfuric acid, in the ratio of 1:3. The second method involved cleaning by O_2 Plasma on PVA TePla PS210 Microwave Plasma System. Contact angle measurements were taken for both sample cleaning methods on a Kruss Easy Drop measurement system. After cleaning by these methods, both samples were settled vertically in a 2.5 wt% aqueous solution of PMMA spheres and withdrawn at a constant rate of ~1.5 mm/hr using a home-made dipping apparatus while subjected to acoustic vibrations through a loudspeaker beneath the solution, this setup is described elsewhere(23, 30).

An aqueous solution of 5 wt% mono-dispersed PMMA spheres, with a diameter of ~700 nm, synthesized with altered concentrations according to the method outlined by Schroden,(31) was mixed with a concentration of 8 mg ml^{-1} surfactant sodium dodecyl sulphate (SDS), a concentration above the theoretical critical micelle concentration (CMC) for SDS of 2.3 mg ml^{-1} (8.0×10^{-3} mol dm^{-3}).(32, 33) Silicon wafer, approximately 1 cm × 1

cm, cleaned in argon plasma and coated with 10 nm titanium adhesion layer and 100-150 nm gold by ion beam sputtering using an Orion-5-UHV, was cleaned by sonication in acetone, ethanol, and rinsed with deionized water and settled vertically in the solution of spheres and withdrawn at a rate of 1 mm/min using a MTI Corporation PTL-MM01 Dip Coater apparatus.

Scanning electron microscopy (SEM), performed on a Hitachi S-4800 field emission SEM, was used to characterize the opal templates and visualize the in-plane (top layer) ordering of the samples. Angle-resolved light scattering spectroscopy was conducted in a monochromator-mount configuration on a rotating stage with varying angle of incidence for photonic band gap investigations. Fixed incident angles of 60° or 45° were used for 2D scattering measurements. A white Halogen bulb collimated to a beam diameter of ~ 1 mm was used to illuminate the sample and spectra of the planar diffracted light were collected with an interval of 5° and an angular resolution of 2° using a CCS200 Compact CCD spectrometer in the wavelength range 200 – 1000 nm.

Results and discussion

Figure 1a outlines the template formation on glass substrates for 700 nm PMMA spheres by noise-assisted dip coating. The acoustic vibrations stop the spheres from settling within solution increasing the thickness and adherence of the spheres to the substrates. Fig.1b and 1c outlines the deposition of the spheres by dip coating at a faster rate under the influence of the added surfactant. The formation of the micelles of SDS within solution improve the order observed in the monolayer film. In both deposition methods for the (111) plane is observed parallel to the substrate, this forms preferentially to other planes due to the spheres having the lowest energy (maximum packing) in this arrangement.

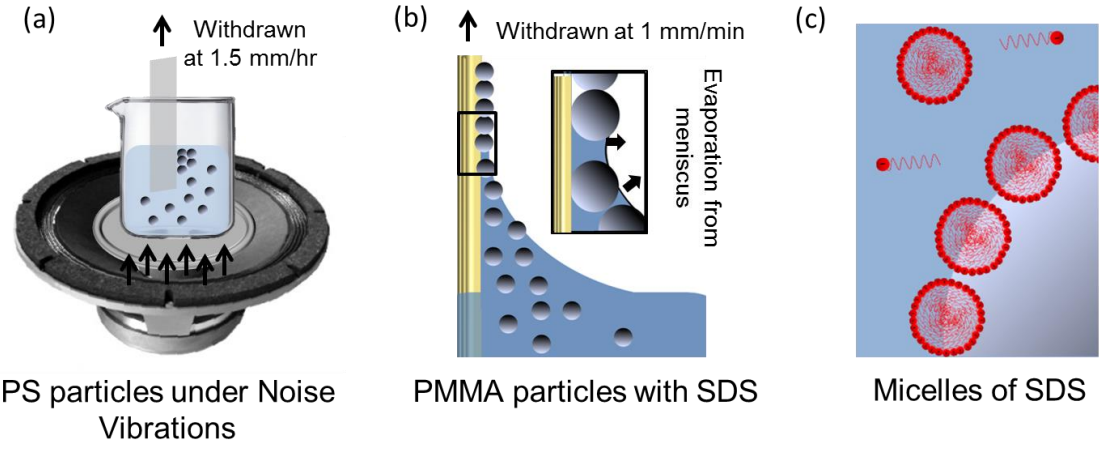

Figure 1. (a) Schematic diagram depicting noise assisted dip coating at ~1.5 mm/hr, and (b) dip-coating of the PMMA spheres at ~ 1 mm/min. (c) Schematic diagram indicating micelle formation of the SDS within solution and interaction with the PMMA sphere surface.

The Piranha cleaned glass produced a substrate with a contact angle of approximately 32.5° and the O_2 plasma clean gave a contact angle of approximately 0°, indicating a more hydrophilic surface, these can be seen in the insets of Figs 2a and d. The sphere template that formed on the Piranha cleaned glass is shown in Figs 2a-c and that formed on the O_2 plasma cleaned glass can be seen in Figs 2d-f. Both samples show fcc ordering in the sphere

arrangement on either surface. The colloidal crystal opal formed on the piranha cleaned glass appears to contain larger scale, but fewer cracks than the O_2 plasma cleaned sample which shows smaller, rounder domains. However, less variation in relative domain orientation is seen on Piranha cleaned substrates (Fig. 2b). Domains with different relative orientations bounded by lateral stacking faults could be seen in the sample formed on the O_2 plasma cleaned substrate in Fig. 2e with a lower sphere concentration. The square packing of the spheres is indicative of a domain with (100) orientation at the surface, while the surrounding areas demonstrate the typical packing with (111) orientation. While Fig. 2b illustrates a number of single-sphere vacancies in the packing order, common in many artificial opals, the film appears more consistently fcc since vacancies do not disrupt the ordering by forming boundaries; rotational and disorder-induced boundaries and domain formation is more prevalent in opals formed on an O_2 plasma cleaned glass. However, both samples have good local crystalline ordering indicated by the FFT of the internal domain structure shown in Figs 2c and f.

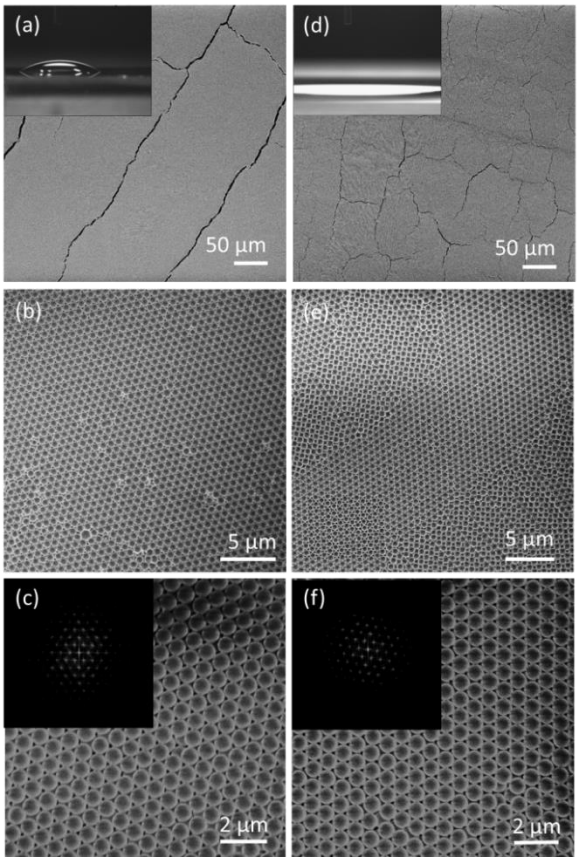

Figure 2. SEM images of inverted opals prepared by noise-assisted dip-coating of 500 nm PS spheres onto glass substrates cleaned by (a-c) Piranha solution and (d-f) O_2 plasma. Inset of (a) shows the contact angle measurement on Piranha cleaned glass and Inset of (d) shows contact angle measurement on O_2 plasma cleaned glass. Inset of (c) FFT of SEM image shown in (c) and Inset of (f) FFT pattern of SEM image in (f).

A photonic bandgap (PBG) was observed for opals grown on the hydrophilized surfaces prepared using both cleaning treatments, confirming 3D order in the assembly of the template. The angle resolved shift in the position of this PBG for different angles of incident light for the sample formed on the Piranha cleaned glass is shown in Fig. 3a and Fig.3b shows the angle resolved shift for the sample on the O_2 plasma cleaned glass. The transmission minimum for the sample on the more hydrophilic surface is deeper than that on

the piranha cleaned glass, in transmission spectra of opals the depth is a function of the disorder with the PBG minima becoming less pronounced with increasing disorder. This serves as an indication of improved order in the sample formed on the more hydrophilic surface.(34)

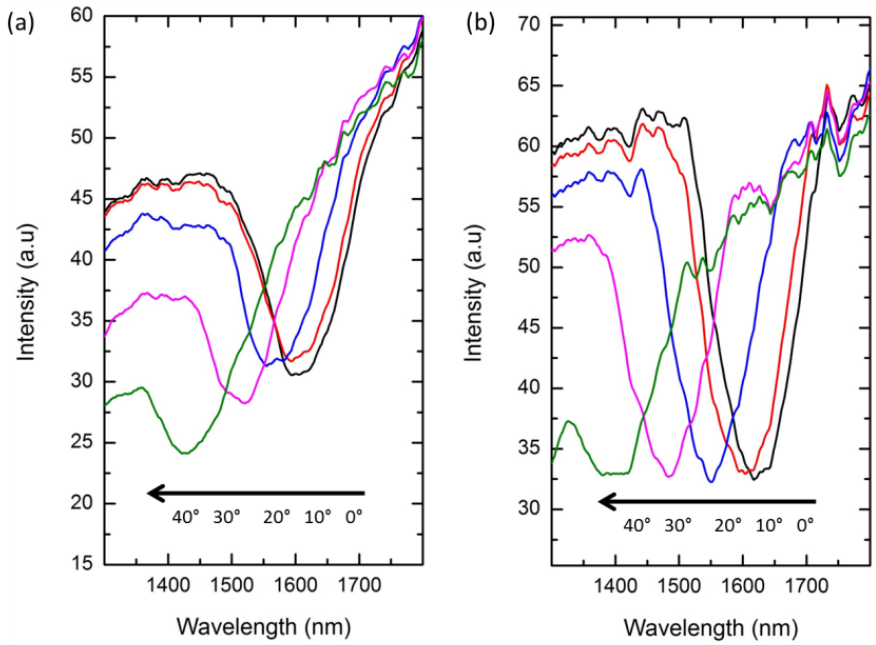

Figure 3. Angle resolved transmission from the template formed on (a) the Piranha cleaned glass and (b) the O_2 plasma cleaned glass.

Fitting of the dispersions for the transmission resonance wavelengths for different planes of the opal lattice for the sample on the more hydrophilic substrate were compared with the Bragg law prediction for a FCC lattice, using the equation $\lambda = 2n_{eff}d_{hkl}\sqrt{(1-(\sin\alpha_{hkl})^2}$ where d_{hkl} is the inter-planer distance for the (*hkl*) planes, n_{eff} is the refractive index, and α_{hkl} is the angle between the incident light and the normal vector to the (*hkl*) plane. A value of n_{eff} = 1.373 and D = 700 nm were used as fitting parameters for calculation of the Bragg fit. This is shown in Fig. 4 whereby the dispersion for the (111) direction fits very well to the theoretical dispersion, but a slight variation is observed for the [11-1] direction, which suggests a variation in the inter-plane distance for this plane.

Therefore, in order to improve deposition on glass substrates, the surfaces should be made as hydrophilic as possible to promote assembly. However, assembly on conductive substrates is more beneficial for many functional materials that rely on a defined template. We next investigated assembly of the spheres on gold coated silicon substrates, and for a method of increasing the rate of withdrawal so as to allow faster dip-coating of the templates. What we observed was at faster rates of withdrawal, far from the equilibrium condition, with non-functionalized spheres such as the PMMA used here, short- and long-range Van der Waals forces(35) dominate over the repulsive interactions of the particles and so there is not sufficient time to achieve the ordered crystallization that does occur using perturbative noise-assisted assembly at much slower rates for these non-functionalized spheres on glass. At the faster rate, with no natural repulsion to assist with ordering, the crystallization inevitably

leads to a disordered and patched coverage of opal deposits on the substrate, particularly for a metallic surface, which has become hydrophobic in air.

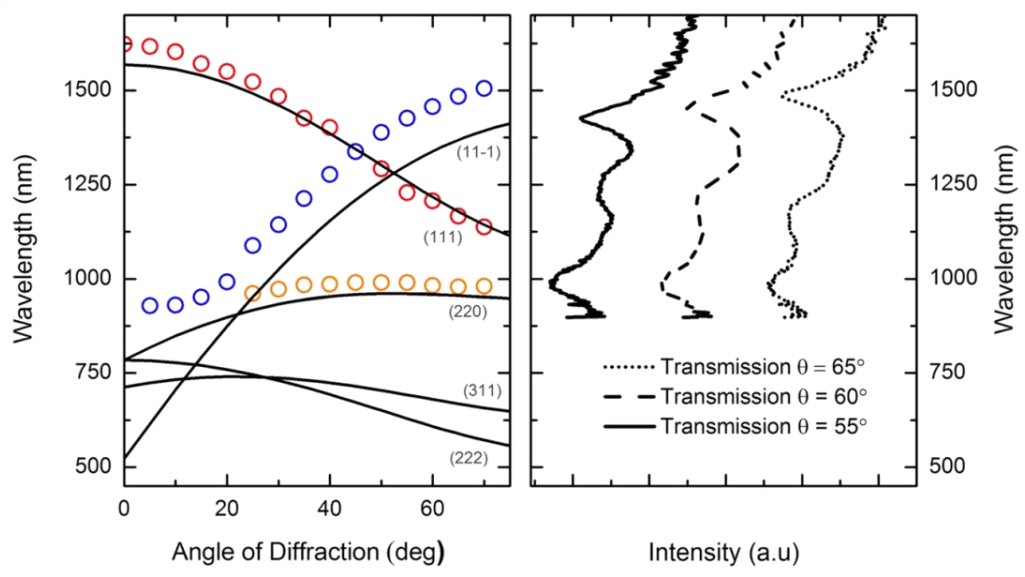

Figure 4. Dispersion of the transmission minima for the sample formed on the O_2 plasma cleaned glass, compared against the theoretical Bragg law dispersions for a 3D photonic crystal with sphere size of 700 nm.

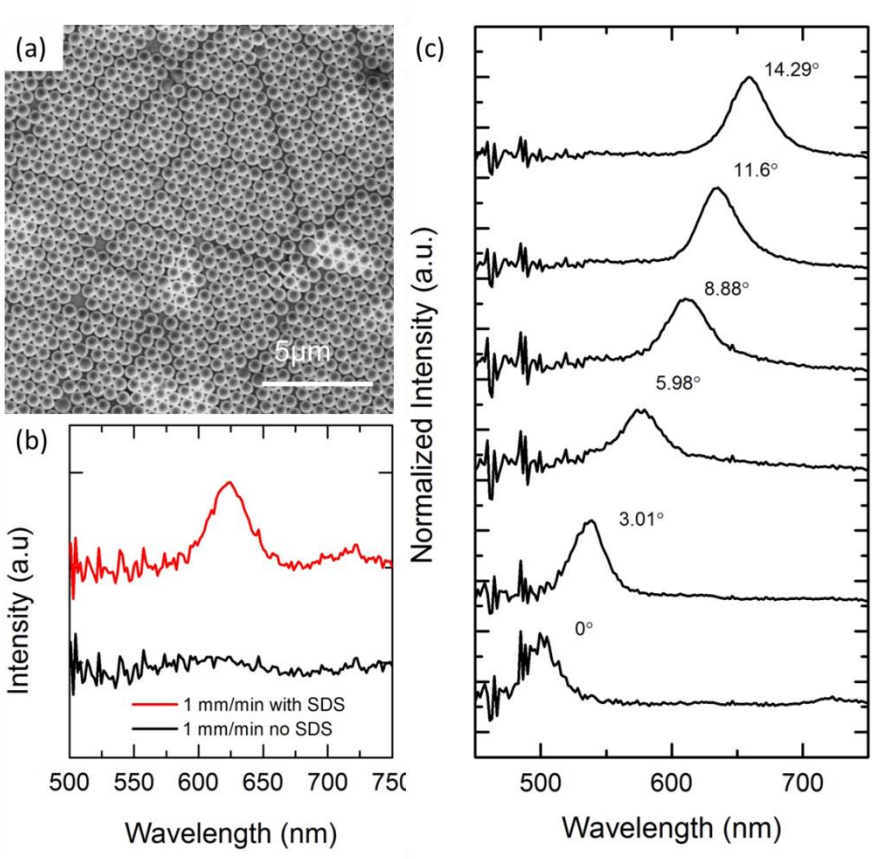

Figure. 5 (a) SEM image of a 2D monolayer photonic crystal formed with 8 mg/ml SDS and 5 wt% PMMA spheres by dip-coating at ~1 mm/min (b) Light scattering normal to the surface (i.e. angle of diffraction = 0°) for light incident at 60°, no peak is visible for a sample formed without SDS (c) Angle resolved scattering from the 2D PhC formed from 5 wt%

PMMA spheres with 8 mg ml^{-1} SDS dip coated at a fast rate (~1 mm/min). Light was incident at 45°.

Without SDS, a monolayer of an amorphous photonic glass is seen to form when withdrawal is of a rate of 1 mm/min for PMMA spheres of 700 nm on the gold surfaces. However, with the addition of the surfactant SDS to the solution of spheres a 2D colloidal crystal monolayer, shown in Fig. 5a, can form with order and quality commensurate with the top surface ordering of multi-layered (3D) deposits observed at the slower rate on glass. SDS dissociates in water to form charged monomers and at a concentration greater than the critical micelle concentration (CMC) of SDS, these monomers orientate their hydrophilic heads towards the polar solute and their hydrophobic tails group together to form micelles. These micelles are known to enhance certain aspects of a solution such as the solubility of hydrophobic materials, and alter other aspects such as viscosity and polarity.(36) Order is thought to be improved via a combination between depletion force kinetics on removal of the spheres from solution and repulsive electrostatic force induced beyond the Debye screening length in the electrical double layer by the SDS. Scattering in the visible range is observed for this ordered sample but not for the sample formed without SDS, shown in Fig. 5b.

The monolayer of spheres formed is of a thickness far below the Bragg attenuation length and so no three-dimensional order is observed, evident by the lack of a PBG. The angular diffraction observed for this sample is shown in Fig. 5c, and this can be used as a measure of the 2D order within the template.

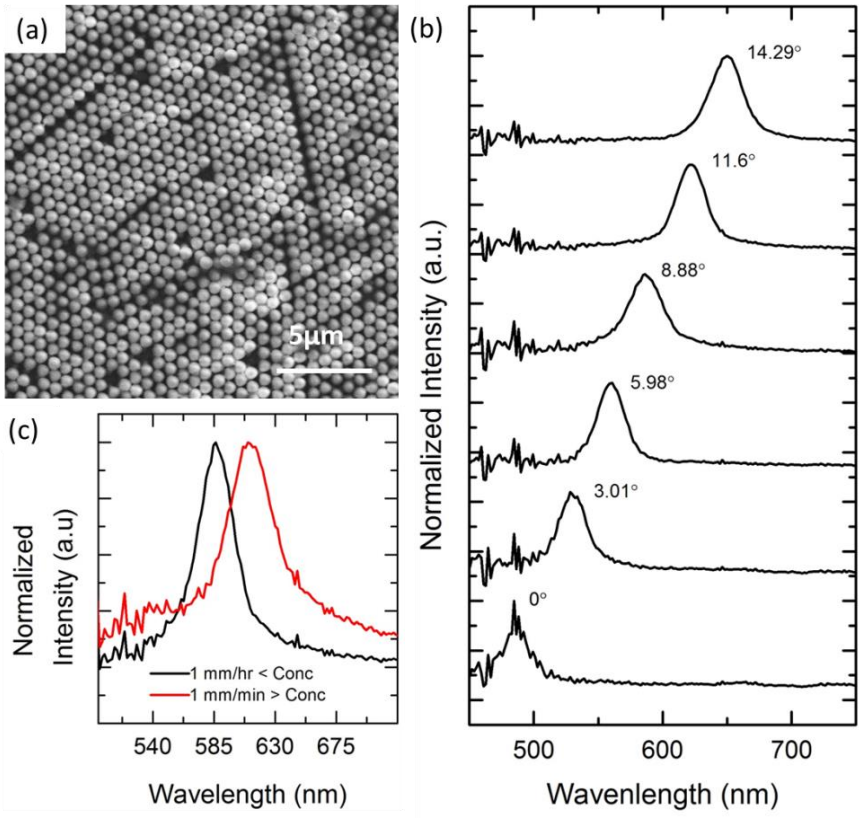

Figure 6. (a) SEM image of a 2D photonic crystal formed with 4 mg/ml SDS and 2.5 wt% PMMA spheres by dip-coating at ~1 mm/hr (b) (b) Angle resolved scattering from the 2D PhC formed from 2.5 wt% PMMA spheres with 4 mg ml^{-1} SDS dip coated at a slow rate (~1 mm/hr). Light was incident at 45° (c) Scattering at an angle of 8.88° for light incident at 45°

for samples formed at fast rate with 5 wt% spheres and 8 mg ml^{-1} SDS (red), and for a sample formed at the slower rate where the concentrations of spheres and SDS are halved (black).

A slower rate of withdrawal from a solution of the same sphere and SDS concentrations produced no ordered opal monolayer but another disordered photonic glass of varying thickness. However, a reduction in sphere concentration by half with a parallel reduction in SDS concentration to 4 mg ml^{-1}, i.e. maintaining the same ratio of spheres to SDS as the fast rate sample, but still above critical micelle concentration resulted in a better quality PhC structure, as shown in Fig. 6a. A similar angular shift of the scattering maxima seen in the 2D opal from the faster rate was observed in this sample as shown in Fig. 6b. A comparison of the scattering of the sample made at the faster rate and at the slower rate but with overall reduced concentration indicates that the slower rate still produces a 2D opal of higher quality than the faster rate but of several more layers than a single monolayer, evident by the sharper peak shown in Fig. 6c, confirmation of increased long-range order for this sample. Where the scattering peak for the fast rate sample is located at a wavelength of $D/\lambda = 1.13$, that of the deposit formed with half the concentration of spheres and SDS at the slower rate is located at $D/\lambda = 1.2$.

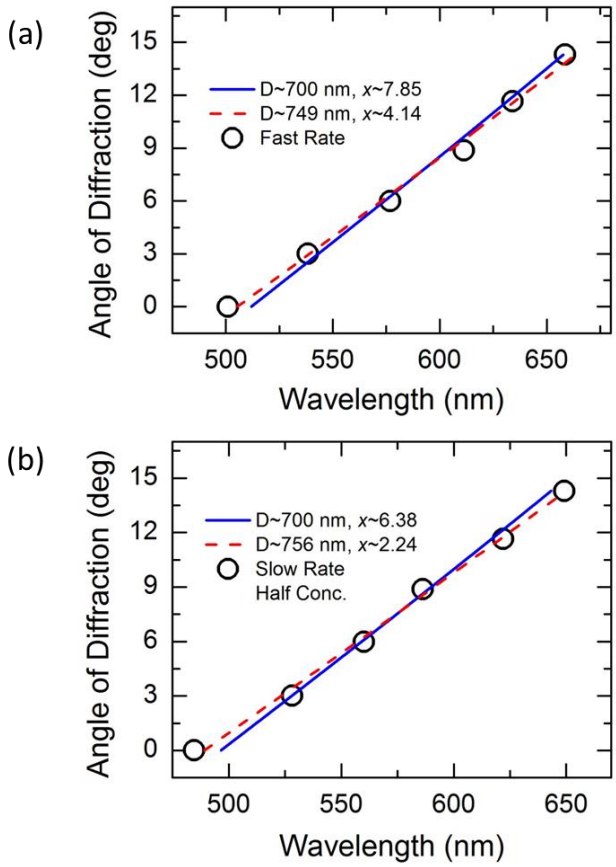

Figure 7. (a) The dispersion of the diffraction maxima for the 5 wt% PMMA sphere and 8 mg ml^{-1} SDS sample withdrawn at a fast rate of withdrawal (~1 mm/min) (b) The dispersion relation for the scattering spectra for the 2.5 wt% PMMA spheres and 4 mg ml^{-1} SDS sample.

The angular dispersion of the diffraction observed from the 2D sample formed with SDS at the faster rate, Fig. 7a, can be fitted to the planar grating equation, $\lambda = d[\sin(\alpha) + \sin(\beta + x)]$, as shown in Fig. 6c, where α is the angle of incidence, β is the angle of diffraction, d is the effective grating groove, which in this case corresponds to $\frac{\sqrt{3}}{2}D$, the half period of the trigonal lattice for the wave vector of incident light propagating along the ΓK direction in the Brillouin zone of a 2D hexagonal lattice. This is represented by the schematic in Fig. 7a, where D is the sphere diameter, and x is the deviation half-angle between incident and diffracted beams defined according to $\alpha(\lambda) = \beta(\lambda) + 2x$. Plotting the angular shift of the diffraction maxima for the slower rate, reduced concentration sample against the theoretical dispersion for a 2D diffraction grating was also conducted as shown in Fig. 7b, confirming the formation of a 2D opal on gold by this slower rate method.

Conclusions

In summary, we prepared 3D photonic crystals on glass of two degrees of hydrophilicity by noise-assisted dip-coating and observed a greater level of long-range order in the film formed on the more hydrophilic substrate. Templates of 700 nm PMMA sphere were then prepared on gold coated silicon substrates by surfactant assisted faster rate dip-coating. The formation of micelles of SDS within solution lead to improved order across a monolayer of PMMA spheres, that behaved as a 2D diffraction grating. The addition of SDS also produced 2D photonic crystals of a greater degree of order and quality at the slower rate on gold substrates, when the concentration of spheres and SDS are both lower but a concentration of SDS above CMC is still maintained. Gold substrates are normally difficult to assemble on at even this slower rate due to the reaction of the substrate with air, and the hydrophobic surface this interaction creates. Therefore with further study surfactant addition to already formed spheres, could be a viable route for improving deposition on metallic surfaces via dip-coating.

Acknowledgments

EA and MO acknowledge the support of the Irish Research Council under awards RS/2010/2920 and RS/2010/2170. WK and CMST acknowledge support from the Spanish National I+D Plan projects TAPHOR (MAT-2012-31392) and CONSOLIDER nanoTHERM (CSD2010-00044). COD acknowledges support from Science Foundation Ireland under award no. 07/SK/B1232a-STTF11, the UCC Strategic Research Fund, and from the Irish Research Council New Foundations Award.

References

1. G. von Freymann, V. Kitaev, B. V. Lotsch and G. A. Ozin, *Chem. Soc. Rev.*, **42**, 2528 (2013).
2. S. M. Doucet and M. G. Meadows, *J. R. Soc., Interface*, **6**, S115 (2009).
3. J. V. Sanders, *Nature*, **204**, 1151 (1964).
4. C. López, *Adv. Mater.*, **15**, 1679 (2003).
5. L. Lu, J. D. Joannopoulos and M. Soljačić, *Phys. Rev. Lett.*, **108**, 243901 (2012).
6. Y. Liu, F. Qin, Z.-Y. Wei, Q.-B. Meng, D.-Z. Zhang and Z.-Y. Li, *Appl. Phys. Lett.*, **95**, 131116 (2009).
7. E. Yablonovitch, *J. Opt. Soc. Am. B*, **10**, 283 (1993).
8. A. Stein, B. E. Wilson and S. G. Rudisill, *Chem. Soc. Rev.*, **42**, 2763 (2013).
9. P. V. Braun, *Chem. Mater.* (2013).
10. J. S. Sakamoto and B. Dunn, *J. Mater. Chem.*, **12**, 2859 (2002).

11. H. Zhang, X. Yu and P. V. Braun, *Nat. Nanotechnol.*, **6**, 277 (2011).
12. N. D. Denkov, O. D. Velev, P. A. Kralchevsky, I. B. Ivanov, H. Yoshimura and K. Nagayama, *Langmuir*, **8**, 3183 (1992).
13. C. Deleuze, B. Sarrat, F. Ehrenfeld, S. Perquis, C. Derail and L. Billon, *Phys. Chem. Chem. Phys.*, **13**, 10681 (2011).
14. A. S. Dimitrov and K. Nagayama, *Langmuir*, **12**, 1303 (1996).
15. M. Pichumani, P. Bagheri, K. M. Poduska, W. Gonzalez-Vinas and A. Yethiraj, *Soft Matter*, **9**, 3220 (2013).
16. P. Jiang, J. F. Bertone, K. S. Hwang and V. L. Colvin, *Chem. Mater.*, **11**, 2132 (1999).
17. A. L. Rogach, N. A. Kotov, D. S. Koktysh, J. W. Ostrander and G. A. Ragoisha, *Chem. Mater.*, **12**, 2721 (2000).
18. M. Bardosova, P. Hodge, L. Pach, M. E. Pemble, V. Smatko, R. H. Tredgold and D. Whitehead, *Thin Solid Films*, **437**, 276 (2003).
19. B. van Duffel, R. H. A. Ras, F. C. De Schryver and R. A. Schoonheydt, *J. Mater. Chem.*, **11**, 3333 (2001).
20. J. R. Oh, J. H. Moon, S. Yoon, C. R. Park and Y. R. Do, *J. Mater. Chem.*, **21**, 14167 (2011).
21. Y. Fu, Z. Jin, Z. Liu, Y. Liu and W. Li, *Mater. Lett.*, **62**, 4286 (2008).
22. K. W. Tan, Y. K. Koh, Y.-M. Chiang and C. C. Wong, *Langmuir*, **26**, 7093 (2010).
23. W. Khunsin, A. Amann, G. Kocher-Oberlehner, S. G. Romanov, S. Pullteap, H. C. Seat, E. P. O'Reilly, R. Zentel and C. M. S. Torres, *Adv. Funct. Mater.*, **22**, 1812 (2012).
24. S. G. Romanov, A. V. Korovin, A. Regensburger and U. Peschel, *Adv. Mater.*, **23**, 2515 (2011).
25. S. G. Romanov, N. Vogel, K. Bley, K. Landfester, C. K. Weiss, S. Orlov, A. V. Korovin, G. P. Chuiko, A. Regensburger, A. S. Romanova, A. Kriesch and U. Peschel, *Phys. Rev. B*, **86** (2012).
26. X. D. Yu, L. Shi, D. Z. Han, J. Zi and P. V. Braun, *Adv. Funct. Mater.*, **20**, 1910 (2010).
27. M. López-García, J. F. Galisteo-López, A. Blanco, J. Sánchez-Marcos, C. López and A. García-Martín, *Small*, **6**, 1757 (2010).
28. T. Smith, *J. Colloid Interface Sci.*, **75**, 51 (1980).
29. W. Khunsin, S. G. Romanov, C. M. S. Torres, J. Ye and R. Zentel, *J. Appl. Phys.*, **104**, 013527 (2008).
30. W. Khunsin, G. Kocher, S. G. Romanov and C. M. S. Torres, *Adv. Funct. Mater.*, **18**, 2471 (2008).
31. R. C. Schroden and N. Balakrishnan, *Inverse Opal Photonic Crystals: A Laboratory Guide*, University of Minnesota Materials Research Science and Engineering Center, University of Minnesota,Amundson Hall 491,421 Washington Ave. SE, Minneapolis, MN 55455 (2001).
32. E. A. G. Aniansson, S. N. Wall, M. Almgren, H. Hoffmann, I. Kielmann, W. Ulbricht, R. Zana, J. Lang and C. Tondre, *J. Phys. Chem.*, **80**, 905 (1976).
33. P. Lianos and R. Zana, *J. Colloid Interface Sci.*, **84**, 100 (1981).
34. S. G. Romanov and C. M. Sotomayor Torres, *Phys. Rev. E*, **69**, 046611 (2004).
35. J. Chen and A. Anandarajah, *J. Colloid Interface Sci.*, **180**, 519 (1996).
36. C. C. Ruiz, *Colloids Surf., A*, **147**, 349 (1999).